Aniline-grafting graphene oxide/polyaniline composite prepared via interfacial polymerization with high capacitive performance

Zhaofen Xu[a,1], Tongzhou Wang[a,1], Liangying Wang[a,1], Jingkun Xu[a], Peipei Liu[a,*], Xiaoqi Lan[a], Xuejing Li[a], Meng Ni[b,*], Qinglin Jiang[c], Fengxing Jiang[a,*]

[a] Jiangxi Engineering Laboratory of Waterborne Coatings, Jiangxi Science & Technology Normal University, Nanchang 330013, China

[b] Department of Building and Real Estate, The Hong Kong Polytechnic University, Hung Hom, Kowloon, Hong Kong China

[c] Institute of Polymer Optoelectronic Materials and Devices, State Key Laboratory of Luminescent Materials and Devices, South China University of Technology, Guangzhou 510640, P. R. China

Corresponding authors. Fax: +86-791-83823320, Tel.: +86-791-88537029

* E-mail: liupeipei8866@126.com (P. P. Liu); meng.ni@polyu.edu.hk(M. Ni); f.x.jiang@live.cn (F. X. Jiang)

[1] Zhaofen Xu, Liangying Wang, and Tongzhou Wang contributed equally.

Abstract

Polyaniline (PANI), a low-cost conductive polymer with an excellent specific capacitance and a high conductivity, is a promising electrode material for supercapacitor. However, it tends to curl and swell after constant charge and discharge, resulting in poor cycle stability. In this work, we employed the interfacial polymerization route to construct an aniline-grafting graphene oxide/polyaniline (GO-ANI/PANI) composite. The as-prepared composite shows a high specific capacitance of 160.5 F g^{-1} at 0.5 A g^{-1} under a wide potential window from 0.0 to 1.0 V. Importantly,

the capacitance retained 86% after 3000 cycles at a high current density of 10 A g^{-1} due to the enhanced interaction between GO and PANI and good conductive network. It has been demonstrated the GO-ANI/PANI composite has a higher specific capacitance and better stability compared to GO/PANI obtained by common method. This study implies that the composite electrode could be a competitive candidate for high performance supercapacitor.

1. Introduction

Clean, efficient and inexpensive energy storage devices are urgently needed to support widespread application of renewable energy and smart grid development.[1,2] As a new type of energy storage device between traditional capacitor and battery, supercapacitor has been applied in various fields in recent years due to its high power density, long cycle life, and friendly environment.[3-5] According to the storage mechanism, supercapacitor can be divided into electrical double-layer capacitor and pseudocapacitor.[6,7] The former stores energy by ion adsorption at the interface formed between electrode and electrolyte, while the latter mainly depends on redox reaction that can offer higher specific capacitance.[8]

The electrode material plays a key role in the performance of supercapacitor, which can be mainly classified into carbon materials, transition metal oxide/hydroxide, and conducting polymers.[9-11] The carbon materials commonly used in supercapacitors include activated carbon, carbon fiber, carbon nanotubes and graphene etc.[12-14] Graphene is a crystalline material arranged along a hexagonal lattice of carbon atoms and extended in two dimensions infinitely, making it endows many excellent properties, such as high electronic conductivity and mechanical strength.[15,16] Therefore, graphene-based materials have attracted increasing attention and been widely employed for energy storage and conversion devices.[17-19] However, the low specific capacitance of graphene-based electrodes for supercapacitors limits its application.

Polyaniline (PANI) as one of excellent conducting polymers is a popular electrode material for pesudocapacitor with high theoretical specific capacitance, low fabrication cost and environmental friendliness.[20,21] Nevertheless, the single PANI electrode suffers from poor cycle stability and low rate capability. Up to now, combining PANI with GO as composite electrode have been confirmed as an efficient method to solve this issue, which could not only make up for the low capacitance of carbon materials but also improve the stability of the conducting polymers.[22-24] For instance, Chen et al[25] prepared rGO/PANI composite electrode by *in situ* one-pot method, retaining 81% of initial specific capacitance after 2000 cycles at a scan rate of 100 mV s^{-1}; Zhou et al[26] reported GO/PANI electrode through *in situ* polymerization with 81% retention after 1000 cylces. Apparently, the cycle stability of GO/PANI-based composite electrodes needed to be further improved, and the synthesis method is relatively complicated. Factually, interfacial polymerization is a simple, controllable, and effective method to produce regular and mass of PANI-based nanofibers compared to other methods,[27-29] which can suppress secondary growth of PANI by removing nanofibers from reactive interface.

Therefore, we synthesized the aniline-grafting graphene oxide/polyaniline (GO-ANI/PANI) composite via the interfacial polymerization process in this work. This kind of the composite have two advantages: on the one hand, the tight interaction between GO and PANI can be enhanced with introduction of the ANI, because GO and ANI are electron acceptor and donor, respectively,[30] which is beneficial for the cycle stability for the composite during continuous charge-discharge process; on the other hand, the presence of the ANI monomer is prone to yield conductive network,[31] facilitating the electron transport. Desirably, the GO-ANI/PANI composite electrode exhibits a high specific capacitance of 160.5 F g^{-1} at 0.5 A g^{-1} and excellent capacitance stability with a retention of 86% after 3000 cycles at 10 A g^{-1}. Furthermore, the GO/PANI composite are also prepared by *in situ* polymerization for comparison to demonstrate the beneficial combination of the GO-ANI/PANI.

2. Experiment

2.1 Materials

Reagent-grade aniline (99.9%, monomer), ammonium persulfate ($[NH_4]_2S_2O_8$, 98%), 1-butyl-3-methylimidazolium hexafluorophosphate, 1-butyl-3-methylimidazolium tetrafluoroborate and 0.22 μm porous polyvinylidene fluoride (PVDF) membrane were obtained from J&K Scientific Co. Aniline was distill-purified. Graphite powder, thionyl chloride ($SOCl_2$), N-Boc-4-aminophenol, trifluoroacetic acid, hydrochloric acid (HCl, 35~37%) and chloroform were purchased from Sinopharm Chemical Reagent Co., Ltd. (Beijing, China). Anhydrous tetrahydrofuran (THF) was distilled prior to usage. All other chemicals were directly used without further purification.

2.2 Preparation of amine-terminated GO (GO-ANI)

GO was obtained according to the modified Hummers method, reported in the literature.[32] 500 mg of well ground GO was added into a two-neck 100 mL round flask charged with a stir-bar. Excess amount of $SOCl_2$ (30 mL) was injected by syringe with stirring under a nitrogen atmosphere, and then heated to 85 °C for refluxing for 24 h to convert the surface-bound carboxylic acids to acyl chlorides. The vent was connected with a $CaCl_2$ guard tube to prevent the resultant from hydrolysis. At the end of acyl chlorination reaction, the residual $SOCl_2$ was removed by distillation under reduced pressure at 80 °C. The obtained solid was immediately dispersed in anhydrous THF (40 mL) and further reacted with 4-N-Boc-aminophenol (0.5 g) under nitrogen protection. After refluxing 12 h at 80 °C, the resultant was cooled to room temperature to collect the solids. The solid products were washed with trifluoroacetic acid (30 mL) for deprotection of the N-Boc groups and subsequently filtrated through 0.22 μm porous PVDF membrane. The filtrated cake was washed with methanol and dried in vacuum dry oven at room temperature for 24 h and the as-obtained powder is assigned as GO-ANI.

2.3 Preparation of GO/PANI composites

The GO-PANI composites were prepared by *in situ* polymerization. Firstly, the 100 mg GO were dispersed into deionized water and ultrasonicated 30 mins to obtain 100 mL homogeneous dispersion in a 250 mL beaker. Then, 100 mL of 8 mM ANI in 1 M HCl was dropped into the beaker. After ultrasonication, the suspended mixture was stirred for 24 h after the addition of $[NH_4]_2S_2O_8$ and HCl. The filtrate cake was washed several times with alcohol, deionized water, and dispersed in deionized water finally.

The PANI nanofiber was prepared using the method demonstrated by Chiou.[33]

2.4 Preparation of GO-ANI grafting polyaniline (GO-ANI/PANI) composites

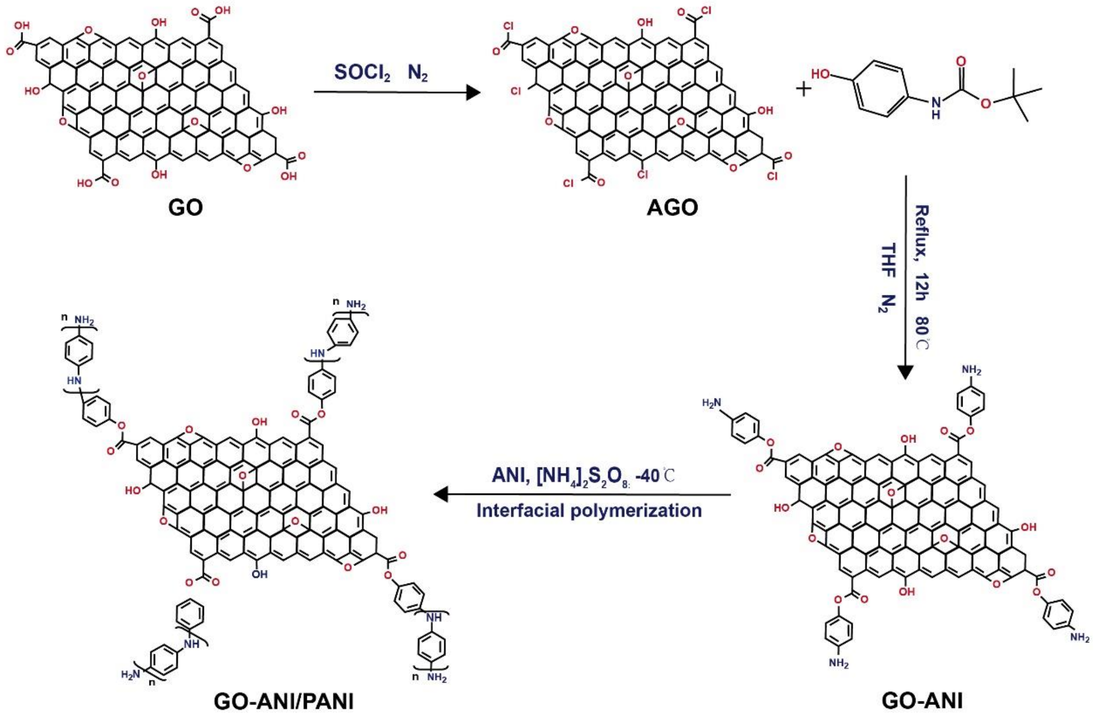

Scheme 1. Schematic illustration of the prepared GO-ANI/PANI composite.

The whole process of GO-ANI/PANI composite is depicted in Scheme 1. GO-ANI/PANI was prepared via an *in situ* low-temperature interfacial polymerization with ANI as a monomer. The detailed designated GO-ANI powder was dispersed into 6 mL of 3 M HCl and ultrasonicated 30 min to obtain a homogeneous dispersion in a 20 mL glass vial. Then 0.1 mL ANI was added to form an aniline/GO-ANI/HCl suspension, followed by moderate stirring for 30 min. After that, 3 mL chloroform was added to the mixture, forming an aqueous/organic interface (*vol./vol.* = 2:1, aqueous phase on the top and chloroform phase at the bottom). This bi-phase suspension was kept at a temperature below –10 ºC with continuous stirring. Then, a freshly prepared solution of $[NH_4]_2S_2O_8$ in 3 M HCl was drop-wisely added into the vial and stirred at –40°C for

24 h, giving rise to the low-temperature interfacial in situ polymerization. In all reactions, the molar ratio of $[NH_4]_2S_2O_8$ to ANI was 10 to 1. After a short induction period ranging from 1 min to several minutes, the dark suspension became green at the interface, indicating a good initiation of polymerization, maintained a proper polymerization in a low-temperature. Along with the reaction, the color of the organic phase became darker, while the aqueous phase turned into shallow. After polymerization, the dark green resultant was filtered through 0.22 μm porous PVDF membrane and washed with deionized water and ethanol several times to remove residual monomer and oxidant. Finally, the filtrated cake was dried in vacuum overnight and denoted to beGO-ANI/PANI. As the initial weight ratio of GO-ANI to ANI was 10:1, 5:1, 1:1 and 1:10, the obtained products were denoted as GO-ANI/PANI-1, GO-ANI/PANI-2, GO-ANI/PANI-3 and GO-ANI/PANI-4, respectively. The pure PANI were synthesized via the same method described above without any GO-ANI into bi-phase suspension before polymerization.

2.5 Characterization and measurements

Raman spectra of composites were collected using a micro-Raman spectrometer (Renishaw, InVia Microscope) with a 532 nm laser. Scanning electron microscopy (SEM) images were recorded by Hitachi-S4800 microscope. Transmission electron microscopy (TEM) images were obtained on FEI TECNAI G2 F20 microscope at an acceleration voltage of 200 kV. All the electrochemical characterizations were carried out on electrochemical workstation (CHI660B, Shanghai Chenhua). The specific capacitance (C_s, F g^{-1}) of the electrode material can be calculated by equation (1):[34]

$$C_s = \frac{It}{mV} \qquad (1)$$

where I (A g^{-1}) is the discharged current density and t (s) is the discharge time, respectively. V (V) and m (g) mean the potential window and the total mass of electrode including active material and current collector (carbon cloth), respectively.

3. Results and discussion.

3.1 Characterizations

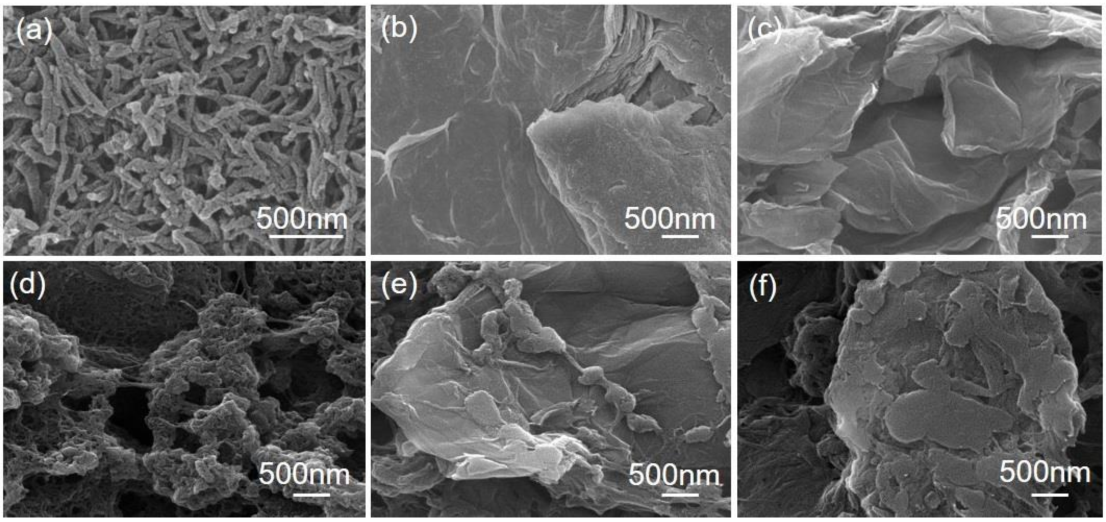

Figure 1. SEM images of (a) PANI, (b) GO/PANI, (c) GO-ANI/PANI-1, (d) GO-ANI/PANI-2, (e) GO-ANI/PANI-3, (f) GO-ANI/PANI-4.

Figure 1 shows the SEM images of PANI and corresponding composite materials. As observed in Fig.1a, the pure PANI electrode presents fine fiber structure. The GO/PANI composite prepared by *in situ* polymerization has a layered outline, while the bare GO shows the sheet structure, as shown in Fig.1b. However, the GO sheet is relatively thick, suggesting that the PANI is hardly inserted during the *in situ* polymerization process. Namely, PANI merely adheres to the surface of GO and can’t substantially change the internal structure of GO attributed to their aggregation during composite process. The GO-ANI/PANI composites prepared by interfacial polymerization, as displayed in Fig. 1(c-f), exhibit the significantly enhanced wrinkle degree with the increase of ANI contents. In addition, the structure of composites by interfacial polymerization are loose and porous liking a sponge derived from the irregular arrangement of PANI, which provides a large number of active sites.[35] This porous structure can facilitate the electrolyte solution enter the interior of the material, which is crucial for the electrode material to store energy.[36]

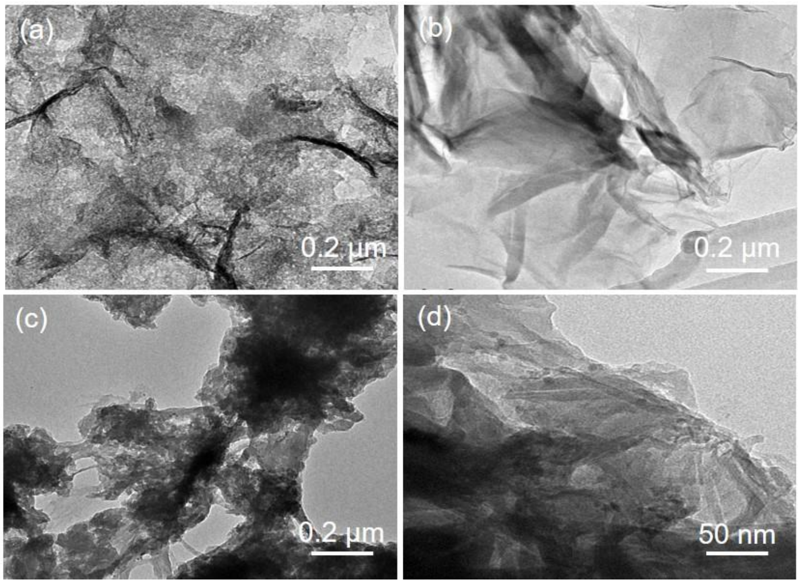

Figure 2. TEM images of (a) GO, (b) GO/PANI and (c, d) GO-ANI/PANI.

Fig. 2a displays the TEM images of GO, revealing its semitransparent, ultrathin, wrinkled, partially curled structure, enabling to collect PANI with sufficient contact area. Moreover, the curl structure with rich wrinkles offers essential resilience and allows the GO-ANI/PANI to have good flexibility. Fig. 2b shows the staggered brightness and darkness of the GO/PANI, which is caused by the uneven distribution of PANI nanofibers on the GO surface. As comparison, closely connected GO with porous structure and PANI nanofibers can be observed for as-prepared GO-ANI/PANI composite in Fig. 2c. During this combination, the ANI monomer plays an important role in interfacial recombination, because it is beneficial for GO-ANI to graft PANI tightly during polymerization process. The high resolution of TEM image in Fig. 2d offers more clear evidence for the as-polymerized PANI nanofibers on the GO-ANI surface. The favorable characteristics of composite also are confirmed by specific surface area and pore size distribution, as exhibited in Fig. S1. As expected, the GO-ANI/PANI shows a large BET specific surface area (19.4 m^2 g^{-1}) with hierarchical porous structures, which is corresponding with these of SEM and TEM analysis.

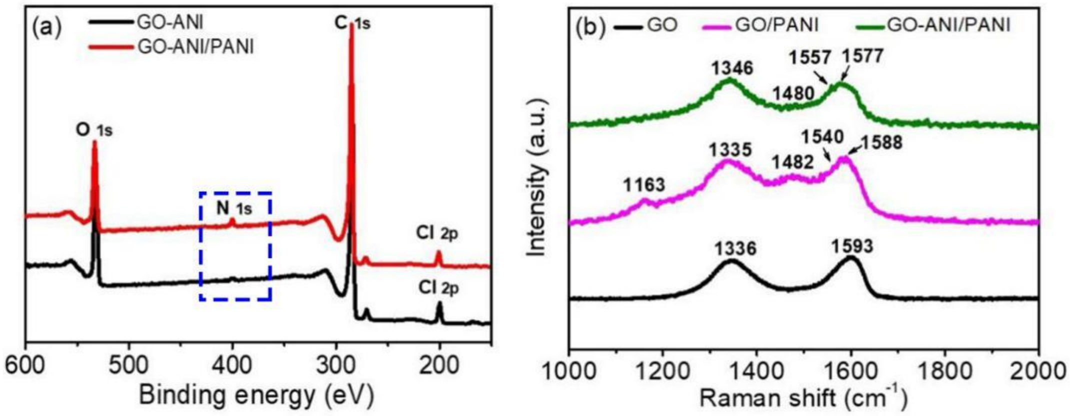

Figure 3. (a) XPS spectra of GO-ANI and GO-ANI/PANI, and (b) Roman spectra of GO, GO/PANI and GO-ANI/PANI.

XPS spectra of GO-ANI and GO-ANI/PANI are shown in Fig. 3. Obviously, the C, O, the presence and N elements can be found in both of the GO-ANI and GO-ANI/PANI composites attributed to the successful combination of ANI and PANI into GO. Noted that, the N element in GO-ANI has a smaller content compared to GO-ANI/PANI, indicating the successful function of ANI group in GO. Moreover, the ANI monomers have been polymerized and the GO-ANI/PANI composites have been obtained successfully. Additionally, Cl element has been also detected in these two samples, which is ascribed to the dope of anions of PANI. Fig. 3b displays the Raman spectra of GO, GO/PANI, and GO-ANI/PANI. The spectrum of GO shows two prominent peaks at 1338 and 1593 cm^{-1}, corresponding to the D and G bonds, respectively.[37,38] For GO/PANI composite, there are several new prominent peaks compared to GO. The bands at 1164, 1337, 1482 and 1583 cm^{-1} are assigned to C−H bending of the quinoid ring, C−N^{+} stretching vibration, C=C vibration of the quinoid rings, and C−C stretching of the benzenoid ring, respectively,[39,40] further indicating the successful combination of PANI in GO.

3.3 Electrochemical performance

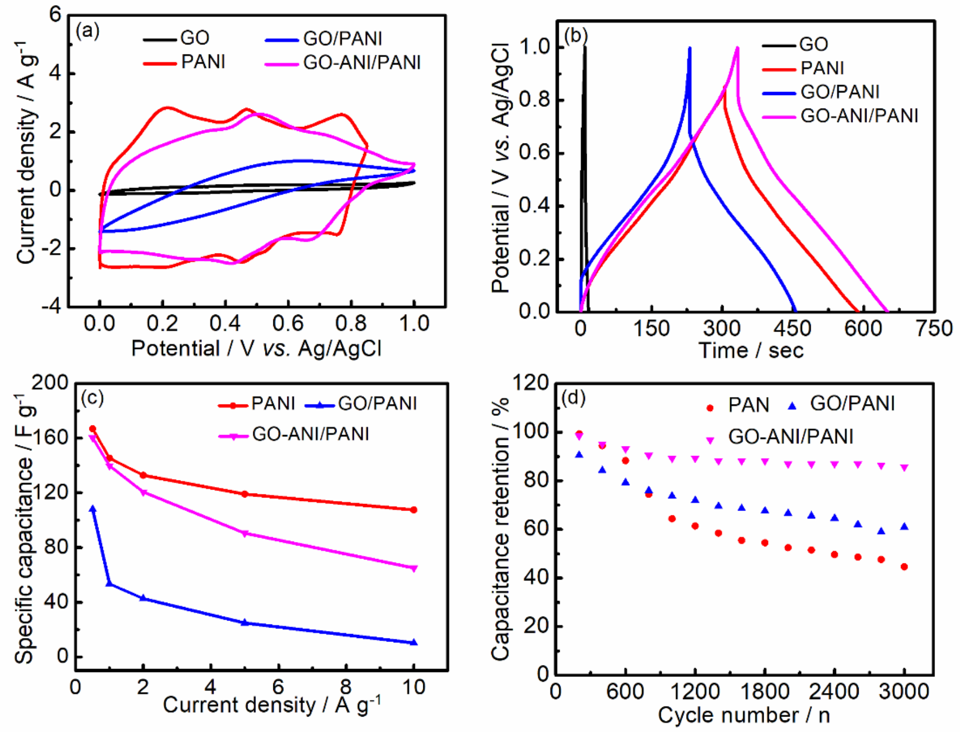

Figure 4. Electrochemical performance of GO, PANI, GO/PANI and GO-ANI/PANI: (a) CV curves at a scan rate of 10 mV s^{-1} and (b) GCD curves at a current density of 0.5 A g^{-1}; (c) specific capacitance at different current densities and (d) cycle stability at 10 A g^{-1}.

The electrochemical behaviors of GO, PANI, GO/PANI and GO-ANI/PANI were measured in 1.0 M H_2SO_4 solution, as shown in Fig. 4. As can be seen from Fig. 4a, the

GO-ANI/PANI electrode shows a large integrated area in CV curve, revealing a higher electrochemical performance compared to GO and PANI at 10 mV s^{-1} under the same potential window from 0.0 to 1.0 V.[41] However, the potential window for the pure electrode PANI is still maintained under a suitable range from 0.0 to 0.8 V with H_2SO_4 as electrolyte, aiming to obtain ideal capacitive performance, which has been confirmed by theoretical calculation and experimental data in many works,[42-44]. The galvanostatic charge-discharge (GCD) curves of these electrodes are measured at a current density of 0.5 A g^{-1}, as shown in Fig. 4b, revealing that PANI and GO-ANI/PANI have longer discharge time than GO and GO/PANI electrodes. To evaluate the electrochemical performance of as-prepared composites, the specific capacitance at different current densities are calculated based on equation (1), as presented in Fig. 4c. The specific capacitance of GO-ANI/PANI (160.5 F g^{-1}) is higher than that of GO/PANI (152.2 F g^{-1}) and comparable to that of PANI (166.8 F g^{-1}) at a current density of 0.5 A g^{-1}. The specific capacitance of GO is only 1.7 F g^{-1} at 0.5 A g^{-1}, as shown in Fig. S2, which is much lower than that of GO-ANI/PANI composite.

Long cycle life is also an important factor to evaluate the practical applications of capacitive electrode. Therefore, the cycle stability of PANI, GO/PANI and GO-ANI/PANI are compared, as displayed in Fig. 4d. The capacitance of GO-ANI/PANI retains 86% after 3000 cycles, while the capacitance of the as-prepared PANI and GO-PANI sharply decrease to 43% and 61%, respectively. Obviously, GO-ANI/PANI prepared by interfacial polymerization can significantly improve the stability of the composite electrode. This can be attributed to the stronger interaction between GO-ANI and PANI than GO/PANI composite. Additionally, the as-prepared GO-ANI/PANI composite shows better capacitive performance and stability than those of previous electrodes, as listed in Table 1.

Table 1 Comparison between the GO-ANI/PANI and reported conducting polymer/graphene oxide composites.

Electrode	Method	Specific capacitance ($F\ g^{-1}$)	Cycle number	Retention	Ref.
G/PANI	*In situ* polymerization	414 ($0.5\ A\ g^{-1}$)	2000	73.5%	[20]
GO/PANI	*In situ* polymerization	199 ($1\ A\ g^{-1}$)	5	85.4%	[45]
PPY/GO	Interfacial polymerization	92.2 ($100\ mV\ s^{-1}$)	*	*	[46]
Sulfonated graphene/PANI	Interfacial polymerization	416 ($30\ mV\ s^{-1}$)	100	77%	[47]
PEDOT/RGO/ MnO_2/Fe_2O_3	Electro-deposition	172 ($100\ mV\ s^{-1}$)	1000	80%	[48]
GO-ANI/PANI	Interfacial polymerization	160 ($0.5\ A\ g^{-1}$)	3000	86%	In this work

The electrochemical behaviors of composite electrode under different initial weight ratio of GO-ANI to ANI are shown in Fig. 5. The GO-ANI/PANI-2 electrode exhibits the best electrochemical activity with apparent redox peaks at 10 mV s^{-1} in Fig. 5a. [23,49] In Fig. 5b, these GCD curves are measured at a current density of 0.5 A g^{-1} under a voltage window of 0-1.0 V. It can be seen that the shapes of these composite materials are similar, and the GO-ANI/PANI-2 shows the longest discharge time. The specific capacitance of GO-ANI/PANI-1, GO-ANI/PANI-3 and GO-ANI/PANI-4 are 100.5 F g^{-1}, 111.4 F g^{-1} and 67.4 F g^{-1}, as shown in Fig. 5c. For comparison, the value of the GO-ANI/PANI-2 is as high as 160.5 F g^{-1} at 0.5 A g^{-1}. One can find, when the weight ratio of GO-ANI to ANI is 5:1, the composite electrode possesses favorable capacitive performance. A suitable ratio of GO-ANI and GO is very important for obtaining a high-quality capacitive material. The fact turns out that the interfacial polymerization is an effective method to enhance the stability of composite.

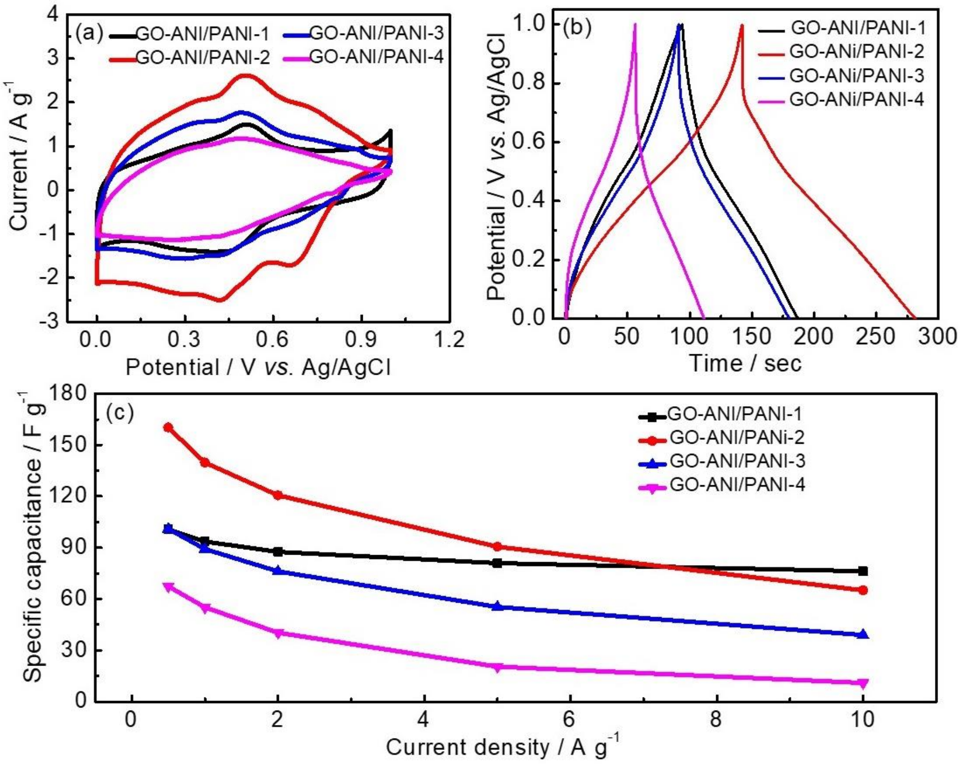

Figure 5. Electrochemical performance of GO-ANI/PANI-1, GO-ANI/PANI-2, GO-ANI/PANI-3 and GO-ANI/PANI-4: (a) CV curves at a scan rate of 10 mV s^{-1} and (b) GCD curves at a current density of 0.5 A g^{-1}; (c) specific capacitance at different current densities.

4. Conclusions

In summary, the aniline-grafting graphene oxide/polyaniline composite as electrode for supercapacitors are constructed through an interfacial polymerization process. The GO-ANI/PANI electrode shows a superior specific capacitance of 160.5 F g^{-1} at the current density of 0.5 A g^{-1} and long-term stability with 86% retention after

3000 cycles. The excellent capacitive behaviors of the composite can be attributed to its strong interaction, unique combination and favorable structure. It turns out that the interfacial polymerization is an effective strategy to fabricate GO-ANI/PANI composite with high electrochemical performance.

Acknowledgements

The authors acknowledge the support by National Natural Science Foundation of China (No.51762018), the Open Fund of the State Key Laboratory of Luminescent Materials and Devices (South China University of Technology, 2019-skllmd-01). M. Ni thanks the funding support from Innovation Technology Fund (Project Number: ITS/026/18) of the Hong Kong Government.

References

[1] Hu CG, Lin Y, Connell JW, Cheng HM, Gogotsi Y, Titirici MM, Dai LM. Carbon-based metal-free catalysts for energy storage and environmental remediation. *Adv Mater*. 2019; 31:1806128.

[2] Lukatskaya MR, Dunn B, Gogotsi Y. Multidimensional materials and device architectures for future hybrid energy storage. *Nat Commun*. 2016; 7:12647.

[3] Liu CC, Yan XJ, Hu F, Gao GH, Wu GM, Yang XW. Toward superior capacitive energy storage: recent advances in pore engineering for dense electrodes. *Adv Mater.* 2018; 30:1705713.

[4] Zhao M, Nie JH, Li H, Xia MY, Liu MY, Zhang ZL, Liang XQ, Qi RJ, Wang ZL, Lu XM. High-frequency supercapacitors based on carbonized melamine foam as energy storage devices for triboelectric nanogenerators. *Nano Energy*. 2019; 55:

447-453.

[5] Guo QF, Li J.J, Zhang B, Guangming Nie GM, Wang DB. High-performance asymmetric electrochromic-supercapacitor device based on poly(indole-6-carboxylicacid)/TiO_2 nanocomposites. *ACS Appl. Mater. Interfaces* 2019; 11:6491-6501.

[6] Zdolsek N, Rocha RP, Krstic J, Trtic-Petrovic T, Sljukic B, Figueiredo JL, Vujkovic MJ. Electrochemical investigation of ionic liquid-derived porous carbon materials for supercapacitors: pseudocapacitance versus electrical double layer. *Electrochim Acta* 2019; 298:541-551.

[7] Zhang W, Jin XZ, Chai H, Diao GW, Piao YZ. 3D hybrids of interconnected porous carbon nanosheets/vertically aligned polyaniline nanowires for high performance supercapacitors. *Adv Mater Interfaces* 2018; 5:1800106.

[8] Lu Q, Chen JGG, Xiao JQ. Nanostructured electrodes for high-performance pseudocapacitors. *Angew Chem Int Ed*. 2013; 52:1882-1889.

[9] Zhang QB, Liu ZC, Zhao BT, Cheng Y, Zhang L, Wu HH, Wang MS, Dai SG, Zhang KL, Ding D, Wu YP, Liu ML. Design and understanding of dendritic mixed-metal hydroxide nanosheets@N-doped carbon nanotube array electrode for high-performance asymmetric supercapacitors. *Energy Storage Mater.* 2019; 16:632-645.

[10] Lyu LL, Chai H, Seong KD, Lee C, Kang J, Zhang W, Piao YZ. Yeast-derived N-doped carbon microshere/polyaniline composites as high performance pseudocapacitive electrodes. *Electrochim. Acta.* 2018; 291:256-266.

[11] Li JJ, Guo QF, Lu Y, Nie GM. Polyindole vertical nanowire array based electrochromic-supercapacitor difunctional device for energy storage and utilization. *Eur. Ploym. J.* 2019; 113:29-35.

[12] Li Z, Liu Z, Sun H, Gao C. Superstructured assembly of nanocarbons: fullerenes, nanotubes, and graphene. *Chem. Rev*. 2015; 115:7046-7117.

[13] Pandolfo AG, Hollenkamp AF. Graphene-based supercapacitor with an ultrahigh energy density. *J. Power Sources.* 2006; 157:11-27.

[14] Yuksel R, Kaplan BY, Bicer E, Yurum A, Gursel SA, Unalan HE. All-carbon hybrids for high performance supercapacitors. *Int. J. Energy Res*. 2018; 42:3575-3587.

[15] Ma WJ, Li M, Zhou X, Li JH, Dong YM, Zhu MF. Three-dimensional porous carbon nanotubes/reduced graphene oxide fiber from rapid phase separation for a high-rate all-solid state supercapacitor. *ACS Appl. Mater. Interfaces* 2019; 11:9283-9290.

[16] Jalili M, Ghanbari H, Bellah MS, Malekfar R. High-quality liquid phase-pulsed laser ablation graphene synthesis by flexible graphite exfoliation. *J. Mater. Sci. Technol*. 2019; 35:292-299.

[17] Xiong R, Hu K, Grant AM, Ma R, Xu W, Lu C, Zhang X, Tsukruk VV. Ultrarobust transparent cellulose nanocrystal-graphene membranes with high electrical conductivity. *Adv. Mater*. 2016; 28:1501-1509.

[18] Bonaccorso F, Colombo L, Yu G, Stoller M, Tozzini V, Ferrari AC, Ruoff RS, Pellegrini V. Graphene, related two-dimensional crystals, and hybrid systems for

energy conversion and storage. *Science.* 2015; 347:1246501.

[19] Mao M, Hu JJ, Liu HT. Graphene-based materials for flexible electrochemical energy storage. *Int. J. Energy Res*. 2015; 39:727-740.

[20] Liu B, Yan J, Gao XG, Huang Y, Zhang YQ. Construction of layer-by-layer sandwiched graphene/polyaniline nanorods/carbon nanotubes heterostructures for high performance supercapacitors. *Electrochim. Acta.* 2018; 272:77-87.

[21] Lin YX, Zhang HY, Liao HY, Zhao Y, Li K. A physically crosslinked, self-healing hydrogel electrolyte for nano-wire PANI flexible supercapacitors. *Chem. Eng. J.* 2019; 367:139-148.

[22] Wu JF, Zhang QE, Wang JJ, Huang XP, Bai H. A self-assembly route to porous polyaniline/reduced graphene oxide composite materials with molecular-level uniformity for high-performance supercapacitors. *Energy Environ. Sci.* 2018; 11:1280-1286.

[23] Sharma K, Pareek K, Rohan R, Kumar P. Flexible supercapacitor based on three-dimensional cellulose/graphite/polyaniline composite. *Int. J. Energy Res.* 2019; 43:604-611.

[24] Hwanga M, Oha J, Kanga J, Seonga KD, Piaoa YZ. Enhanced active sites possessing three-dimensional ternary nanocomposites of reduced graphene oxide/polyaniline/vulcan carbon for high performance supercapacitors. *Electrochim. Acta*. 2016; 221:23-30.

[25] Chen N, Ren Y, Kong P, Tan L, Feng H, Luo Y. In situ one-pot preparation of reduced graphene oxide/polyaniline composite for high-performance

electrochemical capacitors. *Appl. Surf. Sci*. 2017; 392:71-79.

[26] Zhou QH, Wei T, Yue JM, Sheng LZ, Fan ZJ. Polyaniline nanofibers confined into graphene oxide architecture for high-performance supercapacitors. *Electrochim. Acta.* 2018; 291:234-241.

[27] Huang JX, Kaner RB. A general chemical route to polyaniline nanofibers. *J. Am. Chem. Soc*. 2004; 126:851-855.

[28] Zhang QQ, Li Y, Feng YY, Feng W. Electropolymerization of graphene oxide/polyaniline composite for high-performance supercapacitor. *Eletrochim. Acta* 2013, 90:95-100.

[29] QuY, Lu CB, Su YZ, Cui DX, He YF, Zhang C, Cai M, Zhang F, Feng XL, Zhuang XD. Hierarchical-graphene-coupled polyaniline aerogels for electrochemical energy storage. *Carbon* 2018; 127:77-84.

[30] Valles C, Jimenez P, Munoz E, Benito AM, Maser WK. Simultaneous reduction of graphene oxide and polyaniline: doping-assisted formation of a solid-state charge-transfer complex. *J. Phys. Chem. C.* 2011; 115:10468-10474.

[31] Kumar NA, Choi HJ, Shin YR, Chang DW, Dai LM, Baek JB. Polyaniline-grafted reduced graphene oxide for efficient electrochemical supercapacitors. *ACS Nano* 2012; 6:1715-1723.

[32] Zhao X, Zhang Q, Chen D, Lu P. Enhanced mechanical properties of graphene-based poly(vinyl alcohol) composites. *Macromolecules* 2010; 43:2357-2363.

[33] Chiou NR, Epstein AJ. Polyaniline nanofibers prepared by dilute polymerization. *Adv. Mater.* 2005; 17:1679-1683.

[34] Li JP, Xiao DS, Ren YQ, Liu HR, Chen ZX, Xiao JM. Study on the specific capacitance of an activated carbon cloth modified with reduced graphene oxide and polyaniline by cyclic voltammetry. *Electrochim. Acta*. 2019; 30:193-201.

[35] Li X, Zhong Q, Zhang X, Li T, Huang J. In-situ polymerization of polyaniline on the surface of graphene oxide for high electrochemical capacitance. *Thin Solid Films.* 2015; 584:348-352.

[36] Gao Z, Wang F, Chang J, Wu D, Wang X, Wang X, Xu F, Gao S, Jiang K. Chemically grafted graphene-polyaniline composite for application in supercapacitor. *Electrochim. Acta.* 2014; 133:325-334.

[37] Xiang C, Guo RH, Lin SJ, Jiang SX, Lan JW, Wang C, Cui C, Xiao HY, Zhang Y. Lightweight and ultrathin TiO_2-Ti_3C_2TX/graphene film with electromagnetic interference shielding. *Chem. Eng J.* 2019; 360:1158-1166.

[38] Huang L, Chen J, Gao T, Zhang M, Li Y, Dai L, Qu L, Shi G. Reduced graphene oxide membranes for ultrafast organic solvent nanofiltration. *Adv. Mater.* 2016; 28:8669-8674.

[39] Chiou NR, Lu C, Guan J, Lee LJ, Epstein AJ. Growth and alignment of polyaniline nanofibres with superhydrophobic, superhydrophilic and other properties. *Nat. Nanotechnol.* 2007; 2:354-357.

[40] Liao HY, Zhou FL, Zhang ZZ, Yang J. A self-healable and mechanical toughness flexible supercapacitor based on polyacrylic acid hydrogel electrolyte. *Chem. Eng. J.* 2019; 357:428-434.

[41] Yu JH, Xie FF, Wu ZC, Huang T, Wu JF, Yan DD, Huang CQ, Li L. Flexible

metallic fabric supercapacitor based on graphene/polyaniline composites. *Electrochim. Acta.* 2018; 259:968-974.

[42] Li HL, Wang JX, Chu QX, Wang Z, Zhang FB, Wang SC. Theoretical and experimental specific capacitance of polyaniline in sulfuric acid. *J. Power Sources*. 2009; 190:578-586.

[43] Fan LZ, Hu YS, Maier J, Adelhelm P, Bernd Smarsly B, Antonietti M. High electroactivity of polyaniline in supercapacitors by using a hierarchically porous carbon monolith as a support. *Adv. Funct. Mater.* 2007; 17:3083-3087.

[44] Hashemi M, Rahmanifar MS, El-Kady MF, Noori A, Mousavi MF, Kanerde RB. The use of an electrocatalytic redox electrolyte for pushing the energy density boundary of a flexible polyaniline electrode to a new limit. *Nano Energy* 2018; 44:489-498.

[45] Zhang K, Zhang LL, Zhao XS, Wu JS. Graphene/Polyaniline nanofiber composites as supercapacitor electrodes. *Chem. Mater*. 2010; 22:1392–1401.

[46] Bora C, Dolui SK. Fabrication of polypyrrole/graphene oxide nanocomposites by liquid/liquid interfacial polymerization and evaluation of their optical, electrical and electrochemical properties. *Polymer* 2012; 53:923-932.

[47] Hao QL, Wang HL, Yang XJ, Lu LD, Wang X. Morphology-controlled fabrication of sulfonated graphene/polyaniline nanocomposites by liquid/liquid interfacial polymerization and investigation of their electrochemical properties, *Nano Res.* 2011; 4:323-333.

[48] Azman NHN, Sulaiman Y, Mamat@Mat Nazir MS, Lim HN. Novel poly(3,4-

ethylenedioxythiophene)/reduced graphene oxide incorporated with manganese oxide/iron oxide for supercapacitor device. *J. Mater. Sci. Mater. Electron*. 2019; 30:1458-1467.

[49] Male U, Modigunta JKR, Huh DS. Design and synthesis of polyaniline-grafted reduced graphene oxide via azobenzene pendants for high-performance supercapacitors. *Polymer* 2017; 110:242-249.